Journal of Thermal Science Vol.28, No.5 (2019) 875−885

https://doi.org/10.1007/s11630-019-1185-6 **Article ID: 1003-2169(2019)05-0875-11**

A Robust Blade Design Method based on Non-Intrusive Polynomial Chaos Considering Profile Error

GAO Limin[1, 2*], MA Chi[1, 2], CAI Yutong[1, 2]

1. School of Power and Energy, Northwestern Polytechnical University, Xi'an 710129, China
2. The National Key Laboratory of Aerodynamic Design and Research, Xi'an 710129, China

Abstract: To weaken the influence of profile error on compressor aerodynamic performance, especially on pressure ratio and efficiency, a robust design method considering profile error is built to improve the robustness of aerodynamic performance of the blade. The characteristics of profile error are random and small-scaled, which means that to evaluate the influence of profile error on blade aerodynamic performance is a time-intensive and high-precision work. For this reason, non-intrusive polynomial chaos (NIPC) and Kriging surrogate model are introduced in this robust design method to improve the efficiency of uncertainty quantification (UQ) and ensure the evaluate accuracy. The profile error satisfies the Gaussian distribution, and NIPC is carried out to do uncertainty quantification since it has advantages in prediction accuracy and efficiency to get statistical behavior of random profile error. In the integrand points of NIPC, several surrogate models are established based on Latin hypercube sampling (LHS) + Kriging, which further reduces the costs of optimization design by replacing calling computational fluid dynamic (CFD) repeatedly. The results show that this robust design method can significantly improve the performance robustness in shorter time (40 times faster) without losing accuracy, which is meaningful in engineering application to reduce manufacturing cost in the premise of ensuring the aerodynamic performance. Mechanism analysis of the robustness improvement samples carried out in current work can help find out the key parameter dominating the robustness under the disturbance of profile error, which is meaningful to further improvement of compressor robustness.

Keywords: robust design, non-intrusive polynomial chaos, aerodynamic performance, random profile error, uncertainty quantification

1. Introduction

Compressor has the most components in aircraft engine, and its performance is dependent on the blade profile extremely, which means the slight profile deviation will bring out the change of the whole compressor [1]. Due to thin-walled part and the large curve [2], its geometric variability is introduced inevitably in the process of the blade manufacturing process. The profile error distribution of bulk-production blades is uncertain, various and random [3,4] due to positioning, tool wear and material deformation and so on in the blade machining process [5,6]. Some studies show the random and small profile error influences the compressor efficiency

Received: May 07, 2019 Corresponding author: GAO Limin E-mail: gaolm@nwpu.edu.cn

Nomenclature

a	coefficients of NIPC	2D	two-dimensional
C	chord length/mm	CFD	computational fluid dynamics
d	y coordinate distance of control points	LHS	Latin hypercube sampling
E	mean value of variable	MCS	Monte Carlo simulation
e	profile error	NIPC	non-intrusive polynomial chaos
g	random sample in the sample set	NSGA-II	Non-dominated Sorting Genetic Algorithm II
h	the number of samples	NURBS	non-uniform rational B-spline
j	term index of NIPC	Opt	optimal sample
L	thickness	PS	pressure surface
lb	low bound of control points	QoI	quantity of interest
m	the number of integrand points	SS	suction surface
n	the number of uncertain variables	UQ	uncertainty quantification
p	order of NIPC	**Greek symbols**	
Q	the term number of NIPC	β	stagger angle/°
R	control point	π	static pressure ratio
s	index number of samples	σ	standard deviation
t	pitch of the blade/mm	τ	solidity
ub	up bound of control points	Ψ	polynomial basic function
w	weight of polynomial basic function	ϖ	total pressure loss coefficient
X	x coordinate	**Subscripts**	
X/C	normalized x coordinate	Design	Design blade
x	uncertain variable of a system	f	deflection
Y	output of a system	p	pressure
y	y coordinate of control points	s	suction
Abbreviation		y	y coordinate

and stable work range [1,7,8]. The performance can be guaranteed by requiring more severe machining tolerance but accelerated manufacturing cost [9] will be frustrated due to a massive number of blades [10]. Therefore, it is very important to develop robust blade design method considering profile error to trade-off the compressor performance and manufacturing cost.

Robust design method was first proposed by Genichi Taguchi in 1986 to improve the quality of manufactured products by reducing the effect of uncertainties [11]. With the development of robust design method and uncertainty quantification (UQ) method, robust design has been applied in many fields to improve the robustness of products or systems, and many published literatures have showed that such methods managed to get gratifying results [12-16].

Robust design sets mean value (normal value of quantities of interest (QoI)) and variance (fluctuation amplitude of QoI) as its robust design objects. For robust design and robust optimization, many meaningful works have been done to promote the development of it. Andy J. Keane in 2006 proposed robust design method to improve the aerodynamic performance of a compressor fan blade against erosion using Nondominated Sorting Genetic Algorithm II (NSGA-II) and surrogate models which set up with Monte Carlo simulation (MCS) [17]. In the following year, Apurva Kumar realized that the main drawback of direct MCS was the prohibitive computational cost and it was not viable when there was a great amount of candidate designs. For this reason, Bayesian Monte Carlo simulation (BMCS) was proposed by him to improve the computational efficiency in robust design procedures of compressor blades against manufacturing variations [18]. What's more, the efficient Gaussian process emulators introduced in his work was also a main factor for conspicuous computational saving. The same author compared several methods. He concluded that a multi-objective response surface method supported GA performed well in design robust blade in 2009 [19]. And then surrogate models like Kriging and modified ones [20] were introduced in robust design to improve the optimization efficiency. However, the drawback of MCS is computationally expensive which has not been solved fundamentally. For this reason, many researchers propose alternative methods for this problem, such as quadrature methods [21,22], support vector regression (SVR) [23], collocation methods [24,25] and polynomial chaos expansion methods (PCE) [26]. Among these new ideas, PCE stood out because of his high efficiency and accuracy. Zhao set up a robust optimization of airfoil combined with CST parameter-rization and NSGA-II based on non-intrusive polynomial chaos (NIPC) [27], his study showed that the drag coefficient of optimization results was less sensitive to Mach number. In his work, CFD was carried out directly without any surrogate model to ensure the accuracy of uncertainty quantification results. Similar robust design methods based on PCE coupled with a multidisciplinary design optimization (MDO) have been widely applied in industrial engineering, for instance, improving the hovering rotor airfoil under uncertain operating conditions [28] and designing an industrial mixed flow fan resisting erosion [29]. Recently, several works focus on three-dimensional robust optimization design of turbine [30] /compressor [31] blade have been published, which attempted to deal with potential large-scale industrial application problems.

In general, robust design combines a multi-objective optimization method with an uncertainty quantification method, but the views of different researchers are various on the specific methods chosen to perform the robust design. However, they have the same view on this: the efficiency and accuracy of robust design procedure are the key points for each researcher.

According to the above statement, to deal with the effect of geometric variation (especially caused by erosion and manufacturing variations) of blade on its aerodynamic performance, robust design is an acknowledged approach to deal with it. Although many publicshed literatures have proposed a variety of robust design procedures to improve the robustness of blades, the efficiency and accuracy of those procedures are still needed to improve further.

For this reason, a new robust design method is developed based on non-intrusive polynomial chaos (NIPC) in this paper, concentrating on improving the efficiency and accuracy of robust design. This work aims at reducing the sensitivity of aerodynamic performance to profile error.

2. Robust Blade Design Method based on NIPC

2.1 Uncertain profile error and aerodynamic robustness of blade

Profile error (e) is inevitable in the blade machining process due to positioning, tool wear and material deformation and so on. For any qualified bulk-production blades, set s as the index of blades (s =1, …, g, … h), there are profile errors on each of them. The profile error of g_1th and g_2th machined blades (dash-dot-dot lines) are showed in Fig. 1. The dotted line represents design profile line and solid lines represents the tolerance range. All the profile error of machined blades should be in the tolerance range without exception [32]. e_{g_1} and e_{g_2} are the profile error of g_1th and g_2th machined blades, respectively. It means the distance between machined blade profile line and the design profile line. Profile error is a small-scale parameter generated during the process, its distribution satisfied Gaussian distribution [10, 33-36] based on statistical analysis of lots of blades and many published literatures.

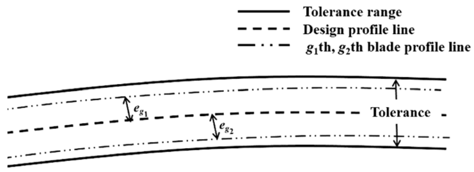

Fig. 1 Tolerance, profile error and design profile line

The profile deviation finally reflects on uncertainty of QoI. There is a ϖ_i (total pressure loss coefficient) [33] and a π_i (static pressure ratio) [37] for each machined blade. For bulk-production blades, the average aerodynamic performances can be expressed by mean value: $E(\varpi)$ and $E(\pi)$. The smaller the difference between the average performance and the original desired design value, the more the designer's idea can be expressed. And the fluctuation of their aerodynamic performance can evaluate by variance $\sigma^2(\varpi)$ and $\sigma^2(\pi)$. The smaller $\sigma^2(\varpi)$ and $\sigma^2(\pi)$, the better the robustness of design blade. Their definitions are in the following formulas (1)-(4):

$$E(\varpi)=\frac{1}{h}\sum_{s=1}^{h}\varpi_s \tag{1}$$

$$E(\pi)=\frac{1}{h}\sum_{s=1}^{h}\pi_s \tag{2}$$

$$\sigma^2(\varpi)=\frac{1}{h-1}\sum_{s=1}^{h}\left(\varpi_s-E(\varpi)\right) \tag{3}$$

$$\sigma^2(\pi)=\frac{1}{h-1}\sum_{s=1}^{h}\left(\pi_s-E(\pi)\right) \tag{4}$$

2.2 Uncertainty quantification based on NIPC

The NIPC belonging to stochastic spectral methods is gradually caught the attention because of the advantages in its prediction accuracy and the efficiency in UQ. For CFD simulations, NIPC can tremendously reduce the simulation number to predict the stochastic output moments [38] compared with classical UQ methods. What's more, NIPC can regard the solving process of

CFD package as a black box without knowing the exact functions. That is the reason why this very method is introduced in this paper.

The main theoretical basis and solving principle of the NIPC are detailed in [39]. For NIPC method, the mean value ($E(Y(x_{m_1}, x_{m_2}, \cdots, x_{m_n}))$) and variance ($\sigma^2(Y(x_{m_1}, x_{m_2}, \cdots, x_{m_n}))$) of the random variable response can be obtained by Eqs. (5) and (6), and the physical meaning of these two parameters are detailed in Section 2.1:

$$E\left(Y\left(x_{m_1}, x_{m_2}, \cdots, x_{m_n}\right)\right) = a_0 \tag{5}$$

$$\sigma^2\left(Y\left(x_{m_1}, x_{m_2}, \cdots, x_{m_n}\right)\right) = \sum_{j=1}^{Q-1}\left[a_j^2\left\langle\psi_j^2\right\rangle\right] \tag{6}$$

$$Q = \frac{(p+n)!}{p!n!} \tag{7}$$

where, $Y(x_{m_1}, x_{m_2}, \cdots, x_{m_n})$ presents the output of a system and $x_{m_i}\,(i=1,\cdots,n)$ are the uncertainty variables, and n is the number of random variables. In this paper, $Y(x_{m_1}, x_{m_2}, \cdots, x_{m_n})$ could be the value of aerodynamic performance parameters (π and ϖ) and x_{m_i} is profile error value at Gaussian Hermite integrand points. ψ_j is j term index of Hermite polynomial of random variables [40], and a_j is the coefficient of NIPC. Q in formula (6) is the number of terms in NIPC. The p in formula (7) is the order of NIPC. This value depends on the accuracy requirement in different cases. For the above formulas, the mean value ($E(Y(x_{m_1}, x_{m_2}, \cdots, x_{m_n}))$) is 0 order term of the coefficient of the polynomial chaos expansion, and the variance ($\sigma^2(Y(x_{m_1}, x_{m_2}, \cdots, x_{m_n}))$) is the quadratic sum of coefficients except a_0. It is easy to know that once the coefficients have been solved, the mean value and the variance are not hard to get. It is needed to note that the way to solve the coefficients is the key point of NIPC. In this paper, the coefficients are calculated by formula (8):

$$a_j = \sum_{m_1=1}^{m}\cdots\sum_{m_n=1}^{m} Y\left(x_{m_1}, x_{m_2}, \cdots, x_{m_n}\right) \frac{\psi_j\left(x_{m_1}, x_{m_2}, \cdots, x_{m_n}\right)}{\left\langle\psi_j\psi_j\right\rangle}\prod_{k=1}^{n} w_{m_k} \tag{8}$$

where, m is the number of integrand points; $w_{m_k}(k=1,2,\cdots,m)$ is weight, which is constant with respect to order of polynomials. The specific calculation method can be found in [40].

2.3 Robust blade design method

The goal of robust design is improving the robustness of product properties when parameters changes randomly. For compressor blade, the robust blade design method considering the profile error aims to enhancing the aerodynamic robustness of compressor blade and reducing its dependency on the blade profile error. Improving the robustness of aerodynamic performance parameters of blades means little changes in E (ϖ) and E (π) or make improvement of these parameters to some extent meanwhile the smaller σ (ϖ) and σ (π), the better. In this paper, the robust design objects are set as finding out minimum E (ϖ) and σ (ϖ); and control variables $\{y_1, y_2, y_3, y_4, y_5, y_6\}$ in formula (9) used to generate new blade samples in the optimization procedure; at the same time, the constraints of this robust blade design method ensures the average aerodynamic performance parameters should not get worse than design value. lb_i and ub_i provide the low bound and up bound of the control points. In the following, this robust blade design method will be introduced in detail.

$$\begin{cases} \text{Objects: } \min\left[E(\varpi), \sigma(\varpi)\right] \\ \text{Variables: } \{y_1, y_2, y_3, y_4, y_5, y_6\} \\ \text{Constraints: } lb_i \le y_i \le ub_i, \\ \qquad E(\varpi) \le E(\varpi)_{\text{Design}}, \\ \qquad E(\pi) \ge E(\pi)_{\text{Desgin}} \end{cases} \tag{9}$$

The entire procedure in this robust design method mainly consists of three parts as showed in Fig. 2: In Part I, parameterizing blade and confirming random profile error distribution; In Part II, training surrogate model; In Part III, optimization method combined with NIPC to get the final optimal samples.

For Part I, parameterization can provide control variables which are used for adding profile error on the design blade. Here, non-uniform rational B-spline (NURBS) is used to parameterize the pressure surface (PS) and suction surface (SS), since NURBS is better at showing blade profile lines than other parameterization methods [41-43]. Confirming the profile error distribution in this part helps to make sure the specific profile error values add to the design blade, which will be used in NIPC as integrand points. Since the profile error satisfied Gaussian distribution as discussed in section 2.1, the integrand points used in NIPC to assess the influence of profile error in this study are based on the integrand points of Gauss-Hermite polynomial.

For Part II, training surrogate models here is a preparation work to save time of optimization in Part III. Generally speaking, surrogate model is used to establish links between input variables and output variables. In present work, directly CFD calculations can totally replace by Kriging models. Kriging model [44, 45] is chosen because it behaves well in building accurate global approximations of a sample space [46]. It should

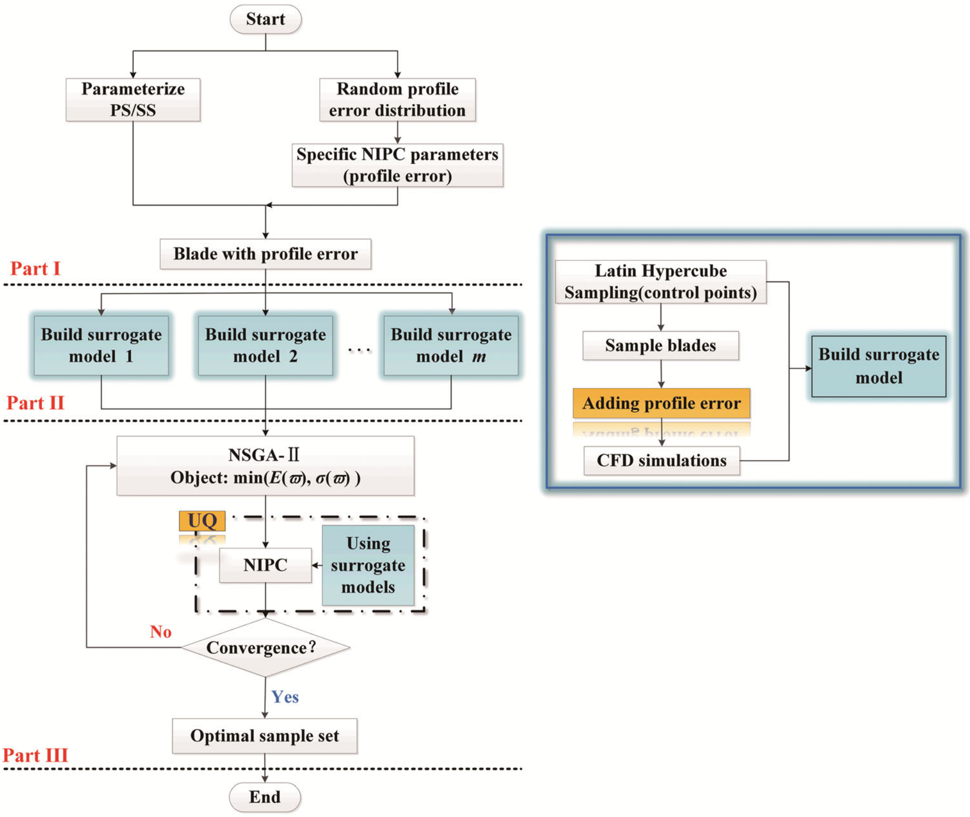

Fig. 2 Procedure of robust optimization design method

be noted that different kinds of surrogate models have been compared and tested beforehand, such as polynomial response surface, radial basis function and Kriging. For the same binary nonlinear function, the prediction results of Kriging are much better than other models but space lacks for a detailed description of it in this paper. All in all, the Kriging surrogate model is sufficient to meet the accuracy requirements of this work. The training random samples for Kriging surrogate model are generated by Latin hypercube sampling (LHS) method [47-49], which has advantage in filling the sample space efficiently and avoid repeating sampling. There are several integrand points used in NIPC as mentioned above. To guarantee the output precision, each integrand point corresponds to a surrogate model instead of one surrogate model for all the integrand points.

For Part III, a multi-objective robust design method is developed for compressor blade. Non-Dominated Sorting Genetic Algorithm (NSGA-II) is employed to find out the optimal robust samples (Pareto optimal set). NSGA-II is able to find much better spread of solutions and better convergence near the true Pareto-optimal front. Aerodynamic performance of all the samples generated in each generation is evaluated by NIPC. It is worth highlighting that NIPC is the key point to improve the efficiency run through this robust design method which shrinks thousand times simulations to several times (based on the order of NIPC). The trained surrogate models in Part II are used here to get the aerodynamic performance of samples and applied to integrand points of NIPC.

Since the object of this method is the robustness of blade aerodynamic performance, the mean value and standard deviation are used as objects in the optimization step. The mean value refers to the average performance of the response and the standard deviation represents how far a set of numbers are spread out from their average value. The smaller the standard deviation, the more robust the performance.

3. Results and Discussion

3.1 Description of geometry and uncertainty

The design blade used here is a two-dimensional (2D) compressor blade. Its chord length (C) is 69.95 mm, solidity ($\tau = C/t$) is 2.3 and stagger angle (β) is 26.58° as shown in Fig. 3. Inflow Mach number is 0.75 and angle of attack is 5°. Random profile error within the tolerance (0.1 mm) satisfied Gaussian distribution [33,50]. Due to the high inflow Mach number, aerodynamic performance is extremely sensitive to geometric shape. The robust design here aims to decrease the sensitivity of aerodynamic performance to geometry.

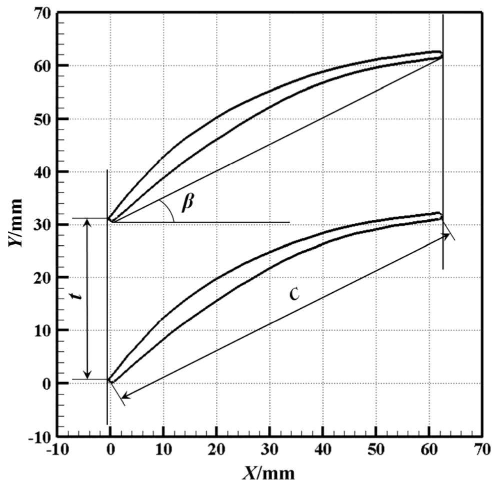

Fig. 3 Geometry parameters of compressor blade

To add profile error to design blade, pressure surface and suction surface both parameterized with eight control points (R_i) by NURBS curve as shown in Fig. 4. And *d* shown in Fig. 4 is the profile error, the new blade profile line is created by translating the y coordinate of design blade control points *d* distance.

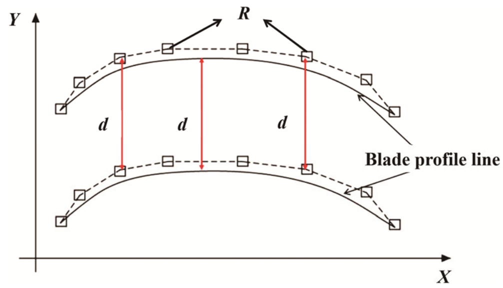

Fig. 4 Construction of profile error

3.2 Validation of NIPC

As mentioned in Section 2.2, the calculation accuracy and calculation time of NIPC are positively related to the order of NIPC. To set the appropriate order for following robust design considering profile error, the 2D blade is used as the research object to compare NIPC results of different orders with MCS on the same computing platform. MCS puts here as reference because it is famous for its solution converging to the exact stochastic solution in UQ. The detail comparisons about the accuracy of $E\ (\varpi)$, $\sigma\ (\varpi)$, $E\ (\pi)$ and $\sigma\ (\pi)$ are discussed in [33] by our research group. With the increase of order of NIPC, the prediction accuracy of these four parameters improved and the prediction result of NIPC is closed to MCS. In addition, the prediction error of NIPC is smaller gradually with the order goes higher. Considering the prediction accuracy and computation cost, the fourth order NIPC method is more appropriate to deal with the profile error problem in this research. Time used by NIPC (4^{th} order, 5 calculation times) is at least 1000 times less than MCS (taking 5000 samples for example), meanwhile, the accuracy satisfies the requirements.

In summary, NIPC method has the advantage of small computation and high prediction accuracy which confront the small-scaled random profile error problem. The application of NIPC in the robust blade design method is a good choice to improve the calculation efficiency substantially.

3.3 Robust design scheme of compressor blade

A robust design is carried out on the 2D blade. In five integrand points of NIPC, it uses LHS to generate 500 initial samples and then call CFD to get aerodynamic performance values to training the Kriging surrogate model, respectively. For NSGA-II, the optimization process of optimum population in this case is decided as 200 and the genetic algebra is 100. The new blades are generated through the changing of control point coordinates (y_i) of camber line and the thickness distribution (ΔL_s, ΔL_P) kept unchanged as shown in Fig. 5. To keep the richness of the optimizing sample space, the disturbance range of the coordinate (y_i) is set as ±10% of the design coordinates. In the meanwhile, the first two and last two comber line control points are kept still to maintain the camber angle same as design blade.

It is worth highlighting that, if going through the whole optimization process without Kriging surrogate models at 5 integrand points, 200×100×5 CFD simulations are needed. When Kriging surrogate models are introduced in, all needed is just 500×5 CFD simulations used for training Kriging models. All in all, the above optimization design scheme can increase the optimization efficiency up to 40 times.

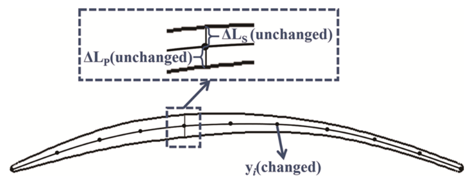

Fig. 5 Generation of new blades

3.4 Robust design results

The geometry of optimized final Pareto solution set (200 samples) is shown in Fig. 6. Overall, the geometry of this set is divided into two groups. The main difference is that the geometric profile curvature change of the front part. Another geometric profile difference of this set located in the range of *X*=57 mm to *X*=61 mm. To analyze the optimization results, two representative samples from Fig. 6 are selected, one sample in each group named as Opt1 and Opt2 shown in Fig. 7, respectively.

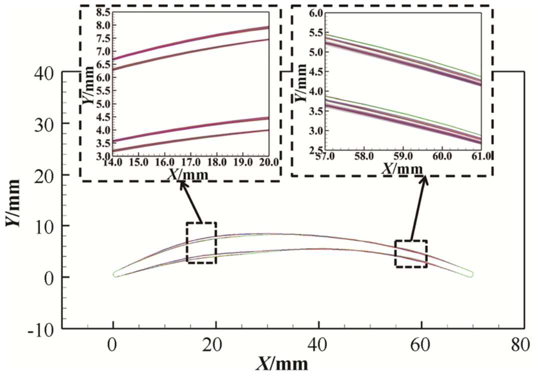

Fig. 6 Final Pareto solution set of blade geometry (200 samples)

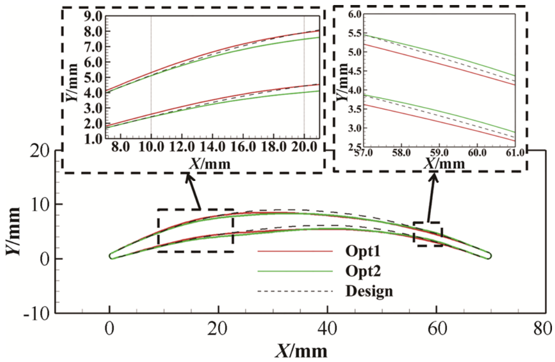

Fig. 7 Optimized blades compared with design

The geometrical characteristics of these two samples compared with design can be clearly seen. In the range of X=0 and X=10 mm, the curvature change of profile line of Opt1 is the largest. The profile line of Opt2 almost coincides with the profile line of the design. In the range of X=10 mm and X=20 mm, the curvature change of Opt2 is smaller than that of design. The curvature change of Opt1 is gradually larger than that of the design. Since then, the curvature change of design keeps larger than those of both Opt1 and Opt2. There is only a short region exception (the profile of Opt2 is higher than the Opt1 and design) between X=57 mm and X=67 mm of Opt2, but this difference is confirmed to be insignificant later. This trend of geometry described above directly affect the statistical characteristics (refer to mean value and standard deviation in current paper) of dynamic performance parameters, which will be discussed in detail in the following sections.

The E (ϖ) and E (π) of the Opt1 and Opt2 compared with the design are presented in Fig. 8. The parameters of optimal samples both satisfy the constraints of NSGA-II, i.e. $E(\varpi) \leq E(\varpi)_{\rm Design}$ and $E(\pi) \geq E(\pi)_{\rm Design}$. As the object, σ (ϖ) of optimal samples are both lower than that of the design, which represents the robustness improvement. It can be concluded from Fig. 8 that the robust design framework is effective to improve the robustness of blade without worsen the average performance value.

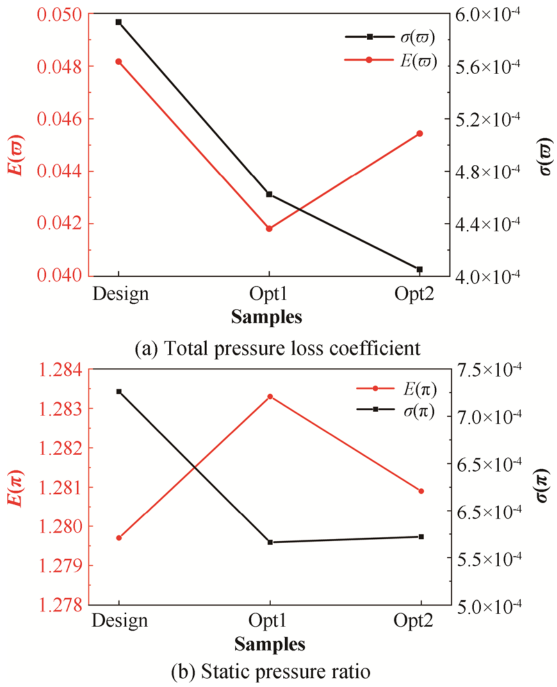

(a) Total pressure loss coefficient

(b) Static pressure ratio

Fig. 8 Overall aerodynamic performance parameter comparison

Comparing the statistical characteristics of optimal samples in Fig. 8(a), E (ϖ) of Opt1 is lower than that of Opt2 while the σ (ϖ) of Opt1 is higher than that of Opt2. In terms of Fig. 8(b), E (π) of Opt1 is higher than that of Opt2 while the σ (π) of Opt1 is lower than that of Opt2. From these comparisons, it can be concluded that the best mean value and standard deviation of some aerodynamic parameter is difficult to concentrate on certain sample. To some extent, the significant improvement in robustness has to sacrifice the mean value. That is to say, there is an unavoidable trade-off has to be made to choose the most suitable sample (proper mean value and standard deviation) among the final optimal geometry set for applied to the real compressor.

The percentage of σ (ϖ) is about 1% of the E (ϖ), which is much higher than the percentage of σ (π). The robustness improvement of ϖ is meaningful in this case. For this reason, the mechanism of σ (ϖ) decrease will be specially concerned and analyzed. Fig. 9 displays total pressure loss coefficient distribution at outlet section of two passages, X/C means normalized pitchwise length. E (ϖ) comparison is showed in Fig. 9(a). The order of maximum value of these three samples is $E(\varpi)_{\rm design} > E(\varpi)_{\rm Opt2} > E(\varpi)_{\rm Opt1}$; the order of pitchwise location of the maximum value of these three samples is $X/C_{\rm design} < X/C_{\rm Opt1} < X/C_{\rm Opt2}$. What's more, the pitchwise scope of ϖ influenced by wake and suction surface boundary layer separation is also a parameter needed to be concerned, which are listed in Table 1. Combined with the data displayed in Fig. 9 and Table 1, Opt1 has advantage in both pitchwise scope of E (ϖ) and maximum E (ϖ).

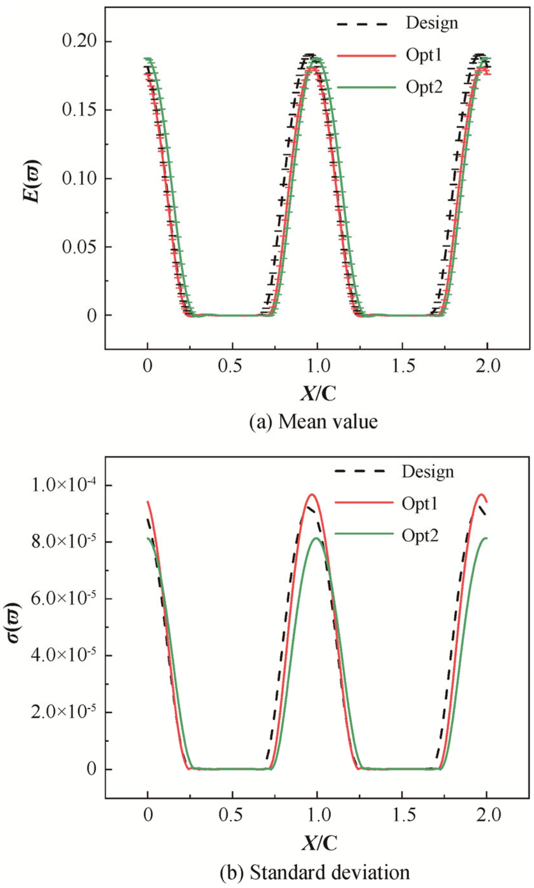

(a) Mean value

(b) Standard deviation

Fig. 9 Total pressure loss coefficient at outlet

Table 1 Pitchwise scope influenced by wake at outlet section

Items	Design	Opt1	Opt2
$E(\varpi)$	55.48%	50.29%	56.53%
$\sigma(\varpi)$	46.12%	41.95%	41.96%

Fig. 9(b) presents σ (ϖ) comparison, the order of pitchwise location of maximum is the same as the location information of E (ϖ), i.e. $X/C_{\text{design}}<X/C_{\text{Opt1}}<X/C_{\text{Opt2}}$. The pitchwise scope and maximum value of σ (ϖ) of Opt2 are both the smallest among these three samples. Although the maximum value of Opt1 is the biggest, the shorter pitchwise scope of σ (ϖ) results in its overall effect of σ (ϖ) is smaller than that of design. The core reason of this distribution will be discussed by E (ϖ) and σ (ϖ) distribution of whole flow field displayed in Fig. 10 and Fig. 11.

According to the E (ϖ) shown in Fig. 10, it can be seen that the main loss sources are the wake and boundary layer separation of suction surface, which have close relationship with the x coordinate of maximum deflection (X_{fmax}, marked with dotted line). Compared with the X_{fmax} of design, the X_{fmax} of Opt1 moves forward while the X_{fmax} of Opt2 moves backward. X_{fmax} guides the boundary layer separation region on suction surface.

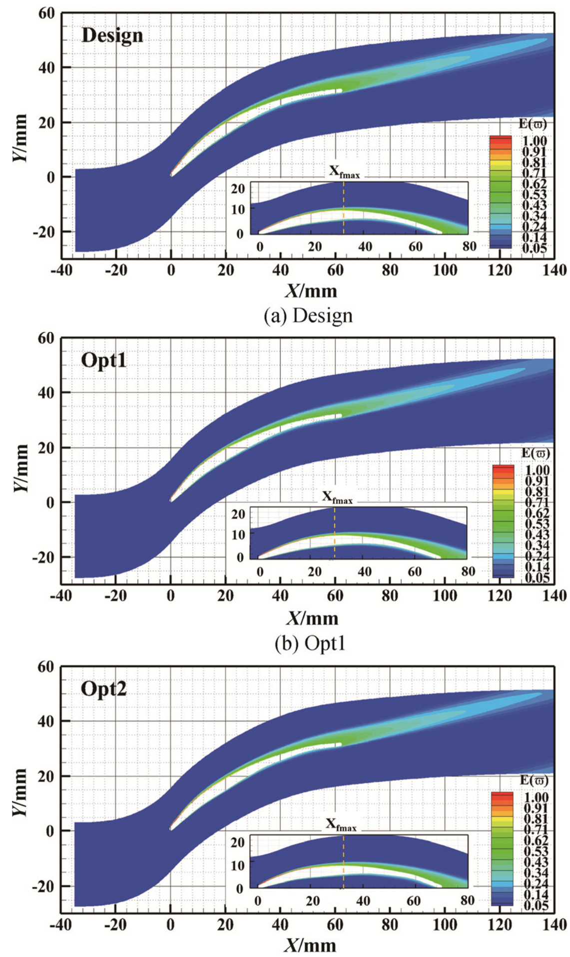

(a) Design

(b) Opt1

(c) Opt2

Fig. 10 Mean value of total pressure loss coefficient of whole flow field

Therefore, X_{fmax} of Opt1 moving forward directly shrink the pitchwise distance of high ϖ at outlet section. In terms of Opt2, although X_{fmax} of Opt2 moving backward is not benefit to reduce ϖ, the flat profile limited the spread of loss along the pitchwise to reduce the total loss.

Fig. 11 shows the σ (ϖ) distributions, which present the fluctuation amplitude of ϖ under the disturbance of profile error. The regions having higher σ (ϖ) in the flow field are the sensitive areas needed to be concerned. The most sensitive regions lies in the wake and related downstream flow field. Compared the Fig. 11(b) and Fig. 11(c) with Fig. 11(a), the sensitive areas have shrunk significantly and fluctuation amplitude for the same location has decreased. The reason is that the boundary layer separation vortex on suction surface of these two optimal samples is compressed compared with the design one in both spanwise and chordwise size. This oblate separation vortex (marked with black frame) helps the main flow reduce disturbance of uncertain profile error. Subsequently, this influence propagating to downstream flow field will weaker.

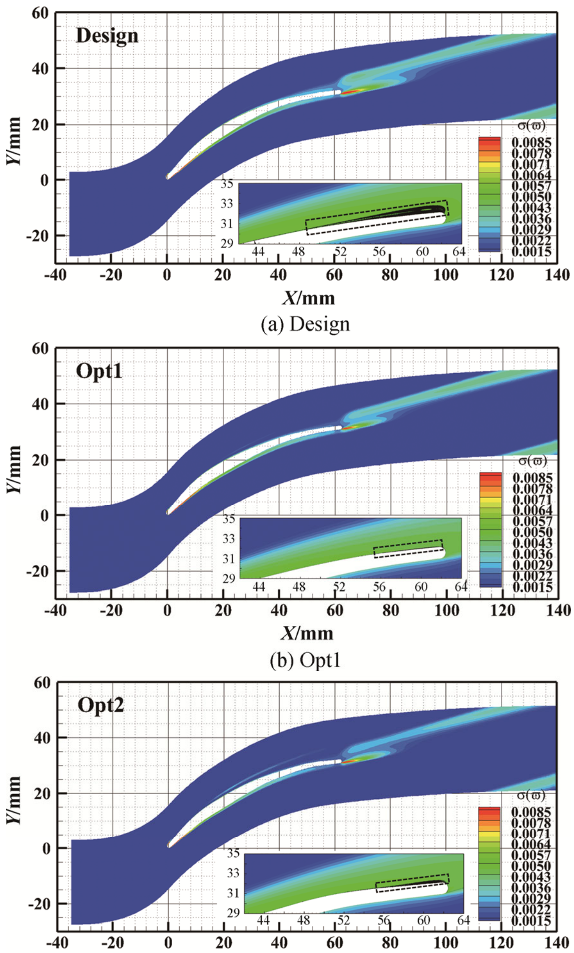

(a) Design

(b) Opt1

(c) Opt2

Fig. 11 Standard deviation of total pressure loss coefficient of whole flow field

4. Conclusions

The influence of profile error uncertainty on aerodynamic performance of compressor blades was studied in this paper. Considering the characteristics of profile error are random and small-scaled, the accuracy and efficiency of the robust design method to deal with a large number of samples with profile error is the core problem. NIPC method was applied to uncertainty quantification and Kriging surrogate model is introduced to reduce CFD simulation time. Those improvements tremendously save design time and get robust blade considering profile error successfully. The conclusions are as follows:

(1) The robust design method which consists of NIPC+ Kriging+ NSGA-II is built and the robust design considering profile error has been conducted. The NIPC method is used in terms of uncertainty quantification to solve the problem of time-consuming and insufficient accuracy. Kriging surrogate model in the optimization process further reduces the computation of optimization.

(2) Based on the established robust design method, the robust design is applied to a two-dimensional blade, which has successfully verified the practical value of the process. The robust design method makes the blade profile being able to maintain good aerodynamic performance under the profile error interference. However, the best values of E (ϖ) and σ (ϖ) cannot be centralized in one sample. There is a trade-off between these two parameters which should be paid attention at compressor blade robust design stage.

(3) Better control of separation vortex on the suction surface is a key point to improve the robustness of blade under disturbance of profile error, since the influence scope of this separation vortex can have significant changes with the profile error.

Acknowledgments

The authors would like to express appreciation for the support of the National Natural Science Foundation of China (NSFC) under the Grant No. 51790512; the Overseas Expertise Introduction Project for Discipline Innovation (111 Project) under Grant No. B17037; Industry-University-Research Cooperation Project of Aero Engine Corporation of China (AECC) under Grant No. HFZL2018CXY011-1 and MIIT.

References

[1] Gao L.M., Cai Y.T., Xu H.L., et al., Uncertainty quantification of airfoil considering manufacturing error. Journal of Aerospace Power, 2017, 32(9): 2253–2259. (in Chinese)

[2] Bolotov M.A., Pechenin V.A., Ruzanov N.V., Uncertainties in measuring the compressor-blade profile in a gas-turbine engine. Russian Engineering Research, 2016, 36(12): 1058–1065.

[3] Chen B., Yang T., Feng T., Ontology-based aero-engine compressor blade manufacturing quality analyzing. International Conference on Computational Intelligence and Software Engineering, IEEE, Wuhan, China, 2009, DOI: 10.1109/CISE.2009.5366278.

[4] Clayton R.D.L., Effects of manufacturing deviation on core compressor blade performance. Virginia Polytechinic Institute and State University, Blacksburg, USA, 2009.

[5] Chen Y., Gao J., Deng H., et al., Spatial statistical analysis and compensation of machining errors for complex surfaces. Precision Engineering, 2013, 37(1): 203–212.

[6] Wang P., Li S., Zhang D., et al., The machining error control of blade shape based on multivariate statistical process control. Proceedings of the Institution of

Mechanical Engineers Part B Journal of Engineering Manufacture, 2015, 229(11): 1912–1924.

[7] Lange A., Voigt M., Vogeler K., Probabilistic CFD simulation of a high-pressure compressor stage taking manufacturing variability into account. ASME Turbo Expo 2010, Power for Land, Sea, and Air, Glasgow, UK, 2010, pp. 617–628. DOI: 10.1115/GT2010-22484.

[8] Gao L. M., Cai Y.T., Zeng R.H., et al., Effects of blade machining error on compressor cascade aerodynamic performance. Journal of Propulsion Technology, 2017, 38(3): 525–531. (in Chinese)

[9] Wang H, Huang L, Yao C, et al., Integrated analysis method of thin-walled turbine blade precise machining. International Journal of Precision Engineering & Manufacturing, 2015, 16(5): 1011–1019.

[10] Eric A. Dow, Wang Q.Q., Simutaneous robust design and tolerancing of compressor blades. Proceedings of the ASME Turbo Expo 2014, Dusseldorf, North Rhine-Westphalia, Germany, 2014, pp. 1–12. DOI: 10.1115/GT2014-25795.

[11] Taguchi G., Elsayed E.A., Hsiang T.C., Quality engineering in production systems. McGraw-Hill, New York, 1989. DOI: 10.1080/00401706.1990.10484745.

[12] Mcallister C.D., Simpson T.W., Multidisciplinary robust design optimization of an internal combustion engine. Journal of Mechanical Design, 2003, 125(1): 39–41.

[13] Khodaygan S., Sharafi M., A new approach for the reliability-based robust design optimization of mechanical systems under the uncertain conditions. SAE Technical Paper, 2018-01-0615.

[14] Wu X., Zhang W., Song S., Robust aerodynamic shape design based on an adaptive stochastic optimization framework. Structural & Multidisciplinary Optimization, 2017, 57(3): 1–13.

[15] David M., Pietro B., Jaikumar L., Carlo L.B., Propagation of uncertainties through wind turbine models for robust design optimization. 35th Wind Energy Symposium, Grapevine, Texas, USA, 2017, pp. 1–10. DOI: 10.2514/6.2017-1849.

[16] Giulia A., Ilya A., Andreas F.B., Robust design optimization of a low pressure turbine rotor discs secondary air system. Proceedings of the ASME Turbo Expo, Charlotte, North Carolina, USA, 2017, pp. 1–12. DOI: 10.1115/GT2017-63289.

[17] Kumar A., Keane A.J., Nair P.B., et al., Robust design of compressor fan blades against erosion. ASME Journal of Mechanical Design, 2006, 128(4): 864–873.

[18] Kumar A., Nair P.B., Keane A.J., et al., Robust design using Bayesian Monte Carlo. International Journal for Numerical Methods in Engineering, 2008, 73(11): 1497–1517.

[19] Keane A.J., Comparison of several optimization strategies for robust turbine blade design. Journal of Propulsion & Power, 2012, 25(5): 1092–1099.

[20] Keane A.J., Cokriging for robust design optimization. AIAA Journal, 2012, 50(11): 2351–2364.

[21] Mattia P., Sergio C.M., Dimitrov G.M., Comparative analysis of uncertainty propagation methods for robust engineering design. Tetrahedron Letters, 2007, 33(43): 6537–6540.

[22] Campobasso M.S., Minisci E., Caboni M., Aerodynamic design optimization of wind turbine rotors under geometric uncertainty. Wind Energy, 2014, 19(1): 1–15.

[23] Smola A.J., Schölkopf B., A tutorial on support vector regression. Statistics and Computing, 2004, 14(3): 199–222.

[24] Loeven G.J.A., Bijl H., Probabilistic collocation used in a two-step approached for efficient uncertainty quantification in computational fluid dynamics. Computer Modeling in Engineering & Sciences, 2008, 36(3): 193–212.

[25] Loeven A., Bijl H., An efficient framework for uncertainty quantification in CFD using probabilistic collocation. 50th AIAA/ASME/ASCE/AHS/ASC Structures, Structural Dynamics, and Materials Conference, Paim Springs, California, USA, 2009, pp. 1–10. DOI: 10.2514/6.2009-2275.

[26] Xiu D., Karniadakis G.E., Modeling uncertainty in flow simulations via generalized polynomial chaos. Journal of Computational Physics, 2003, 187(1): 137–167.

[27] Zhao K., Gao Z.H., Huang J.T., et al., Uncertainty quantification and robust design of airfoil based on polynomial chaos technique. Chinese Journal of Theoretical and Applied Mechanics, 2014, 46(1): 10–19. (in Chinese)

[28] Fusi F., Guardone A., Quaranta G., et al., Multi-fidelity physics-based method for robust optimization with application to a hovering rotor airfoil. AIAA Journal, 2015, 52(11): 1–18.

[29] Wang J., Wen S., Li T., et al., Multidisciplinary design optimization to reduce erosion of blades in a mixed flow fan. Proceedings of the Institution of Mechanical Engineers, Part A: Journal of Power and Energy, 2014, 228(1): 64–82.

[30] Kamenik J., Voutchkov I., Toal D.J.J., et al., Robust turbine blade optimization in the face of real geometric variations. Journal of Propulsion and Power, 2018, 34(6): 1479–1493.

[31] Li Z., Liu Y., Agarwal R.K., Robust optimization design of single-stage transonic axial compressor considering the manufacturing uncertainties. ASME Turbo Expo 2018: Turbomachinery Technical Conference and Exposition. American Society of Mechanical Engineers, 2018 June 11–15, Oslo, Norway, 2018, pp. 1–12. DOI: 10.1115/GT2018-75415.

[32] Lin X.J., Shan C.W., Wang Z.Q., et al., Measurement

techniques of coordinate measuring machine for blade surface of aero-engine. Computer Integrated Manufacturing Systems, 2012, 18(1): 125–131.

[33] Cai Y.T., Gao L.M., Ma C., et al., Uncertainty quantification on compressor blade considering manufacturing error based on NIPC method. Journal of Engineering Thermophysics, 2017, 38(3): 490–497. (in Chinese)

[34] Dow E., Wang Q., The implications of tolerance optimization on compressor blade design. Journal of Turbomachinery, 2015, 137(10): 101008-1–101008-7.

[35] Yan Y., Zhu P.Y., Song L.M., et al., Uncertainty quantification of cascade manufacturing error based non-stationary Gaussian process. Journal of Propulsion Technology, 2017, 38(8): 1767–1775. (in Chinese)

[36] Kumar A., Keane A.J., Nair P.B., et al., Efficient robust design for manufacturing process capability. Proceeding of the 6th ASMO-UK/ISSMO International Conference on Engineering Design Optimization, 2006, pp. 242–250.

[37] Farokhi S., Aircraft propulsion. second ed. West Sussex, John Wiley & Sons Ltd, 2014.

[38] Francesco M., Carnevale M., D'Ammaro A., et al., Uncertainty quantification in computational fluid dynamics and aircraft engines, first ed., Springer International Publishing, Heidelberg, 2015. DOI: 10.1007/978-3-319-14681-2.

[39] Eldred M.S., Burkard J., Comparison of non-intrusive polynomial chaos and stochastic collocation methods for uncertainty quantification. 47th AIAA Aerospace Sciences Meeting Including the New Horizons Forum and Aerospace Exposition, Orlando, Florida, USA, 2009, pp. 1–20. DOI: 10.2514/6.2009-976.

[40] Ouyang J., Numerical analysis, Higher Education Press, Beijing, 2009.

[41] Zhang W., Hao X., Lei H.E., The parametric design of turbine blade based on NURBS. Machine Design & Manufacturing Engineering, 2013, 42(8): 23–26. (in Chinese)

[42] Yang X.D., Bo L., Zhang G.C., et al., Optimization of aspirated airfoil based on artificial bee colony algorithm and NURBS. Journal of Aerospace Power, 2014, 29(8): 1855–1862.

[43] Guo X.Y., Zhang H.J., Dai R., Airship shape optimization with NURBS and gradient based algorithms. Journal of Aerospace Power, 2011, 26(12): 2812–2819.

[44] Sein M. L., Interpolation of spatial data: some theory for Kriging. Springer, New York, 1999.
DOI: 10.1007/978-1-4612-1494-6.

[45] Huang D., Allen T.T., Notz W.I., Zeng N., Global optimization of stochastic black-box systems via sequential Kriging meta-models. Journal of Global Optimization, 2006, 34(2006): 441–466.

[46] Kuhnt S., Steinberg D.M., Design and analysis of computer experiments. AStA Advances in Statistical Analysis, 2010, 94(4): 307–309.

[47] Mckay M.D., Beckman R.J., Conover W.J., A comparison of three methods for selecting values of input variables in the analysis of output from a computer code. Technometrics, 2000, 42(1): 55–61.

[48] Park J.S., Optimal Latin-hypercube designs for computer experiments. Journal of Statistical Planning & Inference, 1994, 39(1): 95–111.

[49] Johnson M.E., Moore L.M., Ylvisaker D., Minimax and maximin distance designs. Journal of Statistical Planning & Inference, 1990, 26(2): 131–148.

[50] Label & tolerance of Blade and airfoil, and surface roughness of blade. Aviation Industry Standard of China, Beijing, China, 1999.